Dispersion- and Exchange-Corrected Density Functional Theory for Sodium Ion Hydration

Marielle Soniat,[†,§] David M. Rogers,[‡,¶,§] and Susan B. Rempe[*,‡]

†*Department of Chemistry, University of New Orleans, 2000 Lakeshore Dr. New Orleans, LA 70148 USA*

‡*Center for Biological and Engineering Sciences, Sandia National Laboratories, Albuquerque, NM 87123 USA*

¶*Current address: Department of Chemistry, University of Florida, Tampa, FL 33610 USA*

§*These authors contributed equally to this work.*

E-mail: slrempe@sandia.gov

Phone: (505) 845-0253

Electronic Supplementary Information

Development of Density Functional Theory

In Kohn-Sham DFT, the energy of the system is based on a mean-field reference system with the same electron density. The energy of the non-interacting part is defined as the sum of the kinetic energy of the electrons, the potential energy (due to the nuclei), and the classical electron-electron repulsion energy. The difference between the reference and fully interacting system is lumped into the exchange-correlation (XC) energy.[1] The true XC functional is unknown and contains the vdW and exchange interactions. An XC functional can be developed as a unit, or exchange and correlation functionals can be developed separately.

The plethora of density functionals is due to the variety of approximate XC functionals.

Early exchange-correlation (XC) functionals were based on the uniform electron gas and called the local spin density approximation (LSDA or LDA). The exchange functional of LSDA can be derived from first principles; the correlation functional is solved numerically.[1]

The next generation of DFs incorporated information about the gradient of electron density at each point via the generalized gradient approximation (GGA). For the exchange functional, most gradient expansions are applicable to slowly varying electron densities (e.g., xPBE, B88). Current implementations focus on the low-gradient limit, which does not describe the electron density properly far from the nucleus where dispersion is important.[1]

GGA correlation functionals are more difficult to develop than the exchange functionals and take a wider variety of approaches. Lee, Yang, and Parr (LYP)[2] based their GGA correlation functional on the Colle-Salvetti formula, originally developed for post-HF theory. Perdew, Burke, and Ernzerhof (cPBE)[3,4] separated the uniform electron gas contribution and the non-uniform contribution. The non-uniform part was then determined by seven physical and mathematical conditions. PBEPBE remains one of the only XC functionals to be determined entirely by theory, with no empirical parameterization.[3]

In a system without dynamical electron correlation, the XC functional should reduce to the exact (HF) exchange functional.[5] Many generalized gradient approximation (GGA) XC functionals, however, do not capture the exact exchange. The adiabatic connection, which links the non-interacting KS reference system with the real system, indicates that mixing HF and DFT exchange is a possible solution to recover exact exchange.[5] Hybrid GGA's introduce a constant amount of HF exchange at all distances.[6] Becke's functionals B3LYP[2,5,7,8] and B97[9] (and its reparameterization B98[10]) belong to this category. B3LYP is one of the most widely used and universally accurate density functionals.[1] Nevertheless, the hybrids do not properly describe dispersion.[11,12]

Criticism of DFT-D

Implementations of DFT-D are criticized on many counts. The higher-order (C_8, C_{10}, ...) and many-body (e.g., C_9) dispersion coefficients are non-negligible in many systems, but neglected in the original DFT-D approach. Determining C_6 from experimental data and keeping C_6 constant in varying atomic coordination states reduces the applicability of the method. DFT-D also introduces additional parameters to the XC functional due to a damping term, which is necessary to prevent divergence of E_{disp} at short range. Lastly, thermochemistry predictions for non-dispersion-bound complexes may deteriorate.[13,14]

Grimme's DFT-D2 scheme[14] addresses some of those concerns by calculating C_6 from theory and reparameterizing B97 with E_{disp} included (B97-D) to improve thermochemistry. Other schemes also include the system dependency of C_6,[15–17] as well as many-body effects.[18] Grimme's DFT-D3 scheme[19] features further improvements by including C_8. Nevertheless, the C_6 value for Na^+, along with the other alkali and alkali earth metals, is arbitrarily set to a small value based on the expectation of low polarizability. The dispersion term may need revision to account for electron delocalization[19] that occurs in coordination complexes, like Na^+-water solvation structures.[20]

Geometry of Optimized Clusters

The thermochemical analysis presented in Sect. 3.4 depends on finding structures that represent a minimum energy geometry for each method. Thus, we reoptimize each structure with each DF to find that DF's minimum-energy structure. For this analysis, we use a correlation-consistent basis set to enhance accuracy (aug-cc-pVDZ).

The lowest-energy coordination structures for $Na^+ \cdot (H_2O)_n$ clusters up to $n = 6$ are similar for all DFs and agree well with previous works (Fig. 2).[21] All methods give reasonable structures for a lone water molecule, with the oxygen-hydrogen bond length (R(O-H)) ranging from 0.961 Å to 0.973 Å and bond angle, θ(HOH), ranging from 104.0° to 105.1°. The distance between the ion and each water molecule in the cluster, R(Na-O), ranges from 2.193

Å to 2.304 Å for $n = 1$ in the DFs, while CCSD gives 2.272 Å. As the coordination number increases from 2 to 6, R(Na-O) distance increases by 0.2 Å. Binding energy and R(Na-O) are correlated for all functionals (Fig. S1), with a linear correlation coefficient of r=0.72. Both R(O-H) and θ(HOH) increase slightly with increasing coordination number, by 0.002 Å and 2°, respectively. More detailed geometry information is contained in Table S3.

CAM-B3LYP consistently produces the shortest ion-water distance, which is 0.07 Å smaller than in the CCSD-optimized structures. Recall that electronic binding energies (ΔE_n) evaluated for CCSD-optimized structures also differ most for CAM-B3LYP relative to CCSD(T) (Sec. 3.1). Those trends indicate enhanced covalency in the Na-O bond for CAM-B3LYP relative to CCSD.

"Split-shell" structures may arise for coordination numbers $n = 5$ and $n = 6$. In that geometry, some waters are directly coordinated to the ion and other waters move to the second solvation shell (e.g., Fig. 2e). We denote these structures as $n = n_{\mathrm{i}} + n_{\mathrm{o}}$, where n_{i} is the number of inner shell waters, directly coordinated to the ion, and n_{o} is the number of second-shell waters. The second-shell waters form hydrogen bonds with the inner-shell waters.[21,22] The outer-shell waters act as double hydrogen bond donors and coordinate with two inner-shell waters. The bond lengths of $\approx$ 1.95 Å and angles of $\approx$ 160° are consistent with Kuo and Mundy's definition of hydrogen bonds.[23]

The ion-oxygen distance for inner-shell waters decreases by <0.01 Å when a second solvation shell is added. Waters in the second solvation shell have θ(HOH) slightly larger than for a lone water molecule. The distance between sodium and the oxygens of the second shell is 4.14 Å in the CCSD/6-31++G** geometry of the $n = 4 + 1$ structures. The ion-water distance for waters of the second solvation shell tends to be shorter for the DFs than CCSD. Again, CAM-B3LYP predicts the shortest ion-water and hydrogen bond distances, indicating more covalency in these bonds. More details of the geometry information on the optimized split-shell structures are contained in Table S4.

Table S1: Parameterization of DF's. Abbreviations are explained below.

DF	Type	Parameters	Training	Basis	Ref.
B3LYP	hybrid GGA[a]	3[b]	G1	_[c]	2,5,7,8
CAM-B3LYP	hybrid GGA + RS	3[d]	G2	aug-cc-pVQZ	6
B97-D	hybrid GGA + D	11	ZT[e], Grim.	TZV2P	14
ωB97X	hybrid GGA + RS	17	CHG[f]	6-311++G(3df,3pd)	25
ωB97X-D	hybrid GGA + RS + D	18	CHG[f]	6-311++G(3df,3pd)	26
B98	hybrid GGA	10	G2	_[c]	9,10
PBEPBE	GGA	0	_[g]	_[c]	3,4
LC-ωPBE	hybrid GGA + RS	3	G2, BH42	6-311+G(3df,2p)[h]	27–29

[a] In some classifications, LYP is a meta-GGA since it depends on the kinetic energy density.

[b] LYP has 4 additional parameters, fit to the He atom.

[c] Developed in a basis set free manner.

[d] The parameters of B3LYP are not readjusted.

[e] MGAE109/3, IP13/3, EA13/3, WI7/05, HB6/04, DI6/04, CT7/04, PPS5/05, HTBH38/04, NHTBH38/04[24]

[f] S22, G3/99 (AE), G2 (IP, EA, PA), NHTBH38/04, HTBH38/04, AE for atoms H through Ar, ZT, dissociation energy of symmetric radical cations (X_2^+, X=H,He,Ne,Ar)[25]

[g] Parameters are set based on physical/mathematical consideration of boundary conditions; no training set was used.

[h] At B3LYP/6-31G(2df,p) geometry.

GGA = generalized gradient approximation; RS = range-separated; D = dispersion corrected

ZT = Zhao and Truhlar; Grim. = Grimme; CHG = Chai and Head-Gordon

Table S2: Details of training sets. Abbreviations are explained below. Most calculated properties are extrapolations to the CCSD(T)/CBS limit.

Set	Interactions	calc./exp.	Ref.
BH42	BH	exp., calc.	[30]
CT7/04	CT	calc.	[31]
DI6/04	DI	calc.	[31]
G1	AE, IP, PA	exp.	[32]
G2	AE, IP, PA, EF	exp.	[33,34]
G3/99	AE, IP, PA, EF	exp.	[35,36]
Grim.	dE, HB, D, EF	exp. (EF only), calc.	[37–39]
HB6/04	HB	calc.	[31]
HTBH38/04	BH	calc.	[40]
NHTBH38/04	BH	exp., calc.	[41,42]
PPS5/05	PP	calc.	[24]
S22	HB, D, CT	calc.	[43]
WI7/05	D	exp., calc.	[31]

AE = atomization energy; IP = ionization potential; PA = proton affinity;
EF = enthalpy of formation; BH = barrier heights;
dE = reaction energy; DI = dipole interaction; PP = $\pi - \pi$ stacking;
HB = hydrogen bonding; D = dispersion; CT = charge transfer;
HTBH = hydrogen transfer barrier heights;
NHTBH = non-hydrogen transfer barrier heights;

Table S3: Geometry of sodium-water clusters including the average sodium-oxygen distance ($R(\mathrm{Na}\cdots\mathrm{O})$), the average bond length of oxygen and hydrogen of the waters (R(O-H)), and average bond angle of water (θ(HOH)) for structures in Figure 2. Clusters were optimized with each method using the aug-cc-pVDZ basis set.

	n	B3LYP	CAM-B3LYP	B98	B97D	ωB97X	ωB97XD	PBEPBE	LC-ωPBE	CCSD
$<\mathrm{R}(\mathrm{Na}\cdots\mathrm{O})>$ (Å)	1	2.216	2.193	2.224	2.304	2.228	2.236	2.224	2.218	2.272
	2	2.237	2.217	2.248	2.337	2.253	2.265	2.250	2.248	2.299
	3	2.268	2.245	2.282	2.374	2.278	2.296	2.279	2.279	2.334
	4	2.300	2.275	2.312	2.413	2.303	2.328	2.313	2.314	2.371
	5	2.361	2.332	2.369	2.467	2.386	2.393	2.380	2.371	2.424
	6	2.422	2.395	2.433	2.513	2.438	2.467	2.448	2.432	2.480
$<$R(O-H)$>$ (Å)	0	0.965	0.963	0.963	0.969	0.961	0.961	0.973	0.962	0.964
	1	0.968	0.966	0.966	0.970	0.964	0.963	0.975	0.965	0.967
	2	0.967	0.966	0.965	0.969	0.964	0.963	0.975	0.965	0.966
	3	0.967	0.965	0.965	0.969	0.963	0.962	0.974	0.964	0.966
	4	0.966	0.965	0.964	0.969	0.962	0.961	0.974	0.963	0.966
	5	0.966	0.965	0.964	0.969	0.963	0.962	0.974	0.963	0.966
	6	0.967	0.966	0.965	0.970	0.964	0.963	0.976	0.965	0.967
$<\theta$(HOH)$>$ (°)	0	104.7	105.1	104.5	104.0	104.8	104.8	103.8	105.1	104.1
	1	104.8	105.0	104.4	104.3	104.6	104.7	104.0	104.8	104.1
	2	104.7	105.0	104.5	104.4	104.7	104.8	104.0	104.9	104.2
	3	104.8	105.1	104.6	104.5	104.8	104.9	104.1	105.1	104.3
	4	104.9	105.3	104.7	104.5	105.0	105.1	104.2	105.2	104.4
	5	105.4	105.8	105.1	105.0	106.1	105.7	104.7	105.7	104.8
	6	106.3	107.0	106.0	105.6	106.7	106.8	106.0	106.7	105.6

Table S4: Geometry of sodium-water clusters including the average sodium-oxygen distance ($R(\mathrm{Na}\cdots\mathrm{O})$), the average bond length of oxygen and hydrogen of the waters (R(O-H)), and average bond angle of water (θ(HOH)) for structures in Figures 2e, 2f, and 2h. Clusters were optimized with each method using the aug-cc-pVDZ basis set.

	$n_i + n_o$	B3LYP	CAM-B3LYP	B98	B97D	ωB97X	ωB97XD	PBEPBE	LC-ωPBE	CCSD
inner shell										
$<\mathrm{R(Na}\cdots\mathrm{O)}>$	4+1	2.296	2.270	2.308	2.403	2.300	2.318	2.310	2.308	2.365
(Å)	4+2	2.294	2.269	2.294	2.396	2.297	2.312	2.308	2.303	2.360
	5+1	2.370	2.347	2.379	2.465	2.386	2.415	2.399	2.378	
$<\mathrm{R(O\text{-}H)}>$	4+1	0.967	0.966	0.966	0.970	0.964	0.963	0.976	0.965	0.967
(Å)	4+2	0.968	0.967	0.968	0.971	0.965	0.964	0.977	0.966	0.967
	5+1	0.968	0.967	0.966	0.970	0.965	0.964	0.977	0.965	
$<\theta\mathrm{(HOH)}>$	4+1	105.6	106.0	105.4	105.2	105.7	105.7	105.0	105.9	105.1
(°)	4+2	106.4	106.8	106.4	105.9	106.3	106.4	105.7	106.6	105.7
	5+1	106.2	106.9	105.9	105.7	106.6	106.7	105.9	106.5	
between shells										
$<\mathrm{R(H}\cdots\mathrm{O)}>$	4+1	1.943	1.905	1.952	1.944	1.909	1.912	1.912	1.943	1.969
(Å)	4+2	1.949	1.911	1.949	1.952	1.915	1.918	1.919	1.949	1.975
	5+1	1.944	1.906	1.955	1.948	1.910	1.909	1.909	1.944	
$<\theta\mathrm{(OH}\cdots\mathrm{O)}>$	4+1	159.0	159.9	159.0	160.7	160.4	160.7	158.8	160.2	159.7
(°)	4+2	159.0	159.7	159.0	160.9	160.5	160.6	158.8	160.1	159.2
	5+1	160.6	161.0	160.6	162.0	161.4	161.9	160.2	161.5	
outer shell										
$<\mathrm{R(Na}\cdots\mathrm{O)}>$	4+1	4.042	4.010	4.057	4.128	4.056	4.056	4.028	4.075	
	4+2		4.055	4.100	4.177	4.105	4.105	4.077	4.118	
	5+1	4.173	4.127	4.191	4.243	4.175	4.175	4.155	4.194	
$<\mathrm{R(O\text{-}H)}>$	4+1	0.967	0.966	0.965	0.970	0.964	0.963	0.975	0.965	0.966
(Å)	4+2	0.967	0.966	0.967	0.970	0.963	0.963	0.975	0.964	0.966
	5+1	0.967	0.966	0.965	0.970	0.964	0.963	0.975	0.965	
$<\theta\mathrm{(HOH)}>$	4+1	105.1	105.6	105.0	104.9	105.3	105.4	104.6	105.5	104.5
(°)	4+2	105.2	105.6	105.2	105.0	105.4	105.5	104.7	105.5	104.6
	5+1	105.1	105.5	105.0	104.9	105.3	105.3	104.5	105.4	

Table S5: Binding energy (ΔE_n) for formation of sodium-water clusters. This table contains the data corresponding to Figure 1.

n		B3LYP	CAM-B3LYP	B97-D	ωB97X	ωB97X-D	B98	PBEPBE	LC-ωPBE	CCSD(T)
1		-24.1	-25.1	-23.2	-23.3	-22.9	-23.8	-23.6	-23.9	-22.6
2		-45.7	-47.7	-44.3	-44.4	-43.6	-45.1	-44.8	-45.3	-42.9
3		-63.2	-66.0	-62.2	-61.7	-60.7	-62.7	-62.3	-62.8	-59.8
4		-77.2	-80.8	-77.1	-76.2	-74.8	-77.0	-76.4	-76.8	-73.8
5		-87.0	-92.0	-89.0	-88.4	-86.0	-87.5	-87.0	-86.9	-84.9
	4+1	-90.3	-95.3	-89.9	-91.5	-89.0	-90.4	-90.3	-89.6	-87.7
6		-96.9	-104.1	-101.9	-102.3	-98.6	-97.8	-98.1	-97.0	-97.8
	4+2	-103.0	-109.4	-102.4	-106.4	-102.7	-103.3	-103.7	-102.0	-101.8

Table S6: Binding enthalpy (ΔH_n°) for formation of sodium-water clusters. This table contains the raw data corresponding to Figure 4.

n		B3LYP	CAM-B3LYP	B97-D	ωB97X	ωB97X-D	B98	PBEPBE	LC-ωPBE	CCSD	Tiss.
1		-23.2	-24.4	-22.3	-22.6	-22.2	-22.9	-22.7	-23.2	-21.7	-25.0
2		-43.2	-45.4	-41.8	-42.1	-41.4	-42.7	-42.2	-43.1	-40.6	-44.8
3		-59.4	-62.6	-58.3	-58.3	-57.9	-59.0	-58.3	-59.3	-56.8	-60.1
4		-72.5	-76.6	-72.2	-71.8	-70.9	-72.3	-71.5	-72.4	-69.2	-73.3
5		-81.2	-86.8	-83.1	-83.8	-81.0	-81.7	-80.9	-81.5		-84.8
	4+1	-84.1	-89.7	-83.7	-86.4	-83.1	-84.1	-84.1	-83.9		-84.8
6		-89.6	-97.6	-94.8	-95.8	-92.0	-90.5	-90.8	-90.6		-95.5
	4+2	-95.3	-102.5	-94.7	-99.4	-95.5	-95.6	-96.3	-95.1		-95.5
	5+1	-91.9	-99.5	-94.2	-97.1	-93.2	-93.2	-93.1	-92.2		-95.5

Table S7: Binding free energy (ΔG_n°) for formation of sodium-water clusters. This table contains the raw data corresponding to Figure 5.

n		B3LYP	CAM-B3LYP	B97-D	ωB97X	ωB97X-D	B98	PBEPBE	LC-ωPBE	CCSD	Tiss.
1		-16.8	-17.8	-16.1	-16.1	-15.8	-16.5	-16.2	-16.7	-15.3	-18.7
2		-30.8	-32.9	-30.5	-29.9	-28.6	-30.7	-30.2	-31.2	-27.8	-31.9
3		-39.4	-42.5	-39.4	-39.2	-36.9	-39.2	-38.5	-39.4	-35.8	-40.9
4		-44.0	-48.7	-45.6	-45.2	-42.1	-44.5	-43.7	-44.9	-43.5	-46.9
5		-42.9	-48.0	-45.8	-42.8	-41.5	-43.7	-42.9	-43.7		-50.5
	4+1	-44.6	-50.0	-45.8	-45.5	-44.2	-45.0	-44.8	-44.6		-50.5
6		-38.2	-44.7	-43.2	-43.3	-40.0	-39.1	-39.0	-39.0		-53.4
	4+2	-44.6	-51.3	-45.7	-49.5	-45.5	-45.1	-45.7	-44.7		-53.4
	5+1	-41.0	-47.2	-44.1	-45.0	-41.7	-41.4	-41.4	-41.2		-53.4

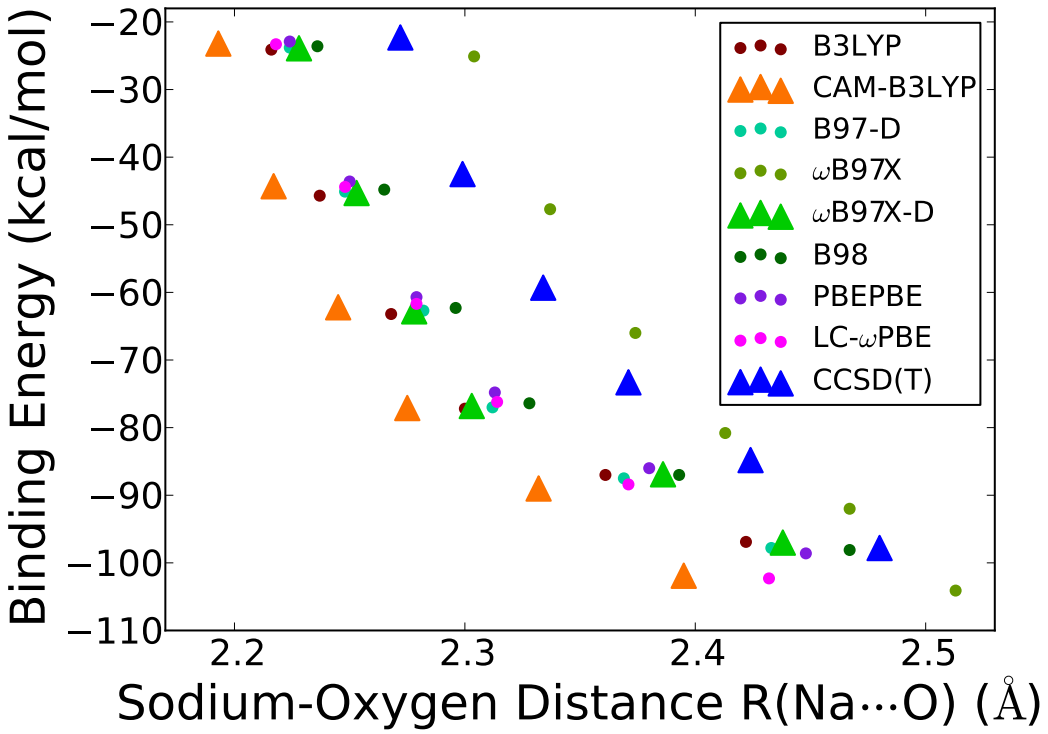

Figure S1: Correlation of the binding energy (ΔE_n) to the average ion-oxygen distance, $< R(\mathrm{Na}\cdots\mathrm{O}) >$, for each DF and CCSD/aug-cc-pVDZ in their optimum geometries (linear correlation coefficient r=0.72). The number of waters in the cluster increase from top to bottom (n=1-6). Units are Angstroms.

References

(1) Cohen, A. J.; Mori-Sanchez, P.; Yang, W. *Chem. Rev.* **2012**, *112*, 289–320.

(2) Lee, C.; Yang, W.; Parr, R. G. *Phys. Rev. B* **1988**, *37*, 785–789.

(3) Perdew, J. P.; Burke, K.; Ernzerhof, M. *Phys. Rev. Lett.* **1996**, *77*, 3865.

(4) Perdew, J. P.; Burke, K.; Ernzerhof, M. *Phys. Rev. Lett.* **1997**, *78*, 1396–1396.

(5) Becke, A. D. *J. Chem. Phys.* **1993**, *98*, 5648–5652.

(6) Yanai, T.; Tew, D. P.; Handy, N. C. *Chem. Phys. Lett.* **2004**, *393*, 51 – 57.

(7) Vosko, S. H.; Wilk, L.; Nusair, M. *Can. J. Phys.* **1980**, *58*, 1200–1211.

(8) Stephens, P. J.; Devlin, F. J.; Chabalowski, C. F.; Frisch, M. J. *J. Phys. Chem.* **1994**, *98*, 11623–11627.

(9) Becke, A. D. *J. Chem. Phys.* **1997**, *107*, 8554–8560.

(10) Schmider, H. L.; Becke, A. D. *J. Chem. Phys.* **1998**, *108*, 9624–9631.

(11) Johnson, E. R.; Mackie, I. D.; DiLabio, G. A. *J. Phys. Org. Chem.* **2009**, *22*, 1127–1135.

(12) Grimme, S. *Wiley Interdisciplinary Reviews: Comp. Mol. Sci.* **2011**, *1*, 211–228.

(13) Klimes, J.; Michaelides, A. *J. Chem. Phys.* **2012**, *137*, 120901.

(14) Grimme, S. *J. Comp. Chem.* **2006**, *27*, 1787–1799.

(15) Tkatchenko, A.; Scheffler, M. *Phys. Rev. Lett.* **2009**, *102*, 073005.

(16) Sato, T.; Nakai, H. *J. Chem. Phys.* **2009**, *131*, 224104.

(17) Becke, A. D.; Johnson, E. R. *J. Chem. Phys.* **2005**, *123*, 154101.

(18) DiStasio, R. A.; von Lilienfeld, O. A.; Tkatchenko, A. *Proc. Natl. Acad. Sci.* **2012**, *109*, 14791–14795.

(19) Grimme, S.; Antony, J.; Ehrlich, S.; Krieg, H. *J. Chem. Phys.* **2010**, *132*, 154104.

(20) Varma, S.; Rempe, S. B. *Biophys. J.* **2010**, *99*, 3394–3401.

(21) Kim, J.; Lee, S.; Cho, S. J.; Mhin, B. J.; Kim, K. S. *J. Chem. Phys.* **1995**, *102*, 839.

(22) Feller, D.; Glendening, E. D.; Woon, D. E.; Feyereisen, M. W. *J. Chem. Phys.* **1995**, *103*, 3526.

(23) Kuo, I.-F. W.; Mundy, C. J. *Science* **2004**, *303*, 658.

(24) Zhao, Y.; Truhlar, D. G. *J. Phys. Chem. A* **2005**, *109*, 5656–5667.

(25) Chai, J.-D.; Head-Gordon, M. *J. Chem. Phys.* **2008**, *128*, 084106.

(26) Chai, J.-D.; Head-Gordon, M. *Phys. Chem. Chem. Phys.* **2008**, *10*, 6615–6620.

(27) Vydrov, O. A.; Heyd, J.; Krukau, A. V.; Scuseria, G. E. *J. Chem. Phys.* **2006**, *125*, 074106.

(28) Vydrov, O. A.; Scuseria, G. E. *J. Chem. Phys.* **2006**, *125*, 234109.

(29) Vydrov, O. A.; Scuseria, G. E.; Perdew, J. P. *J. Chem. Phys.* **2007**, *126*, 154109.

(30) Zhao, Y.; Lynch, B. J.; Truhlar, D. G. *J. Phys. Chem. A* **2004**, *108*, 2715–2719.

(31) Zhao, Y.; Truhlar, D. G. *J. Chem. Theory Comput.* **2005**, *1*, 415–432.

(32) Pople, J. A.; Head-Gordon, M.; Fox, D. J.; Raghavachari, K.; Curtiss, L. A. *J. Chem. Phys.* **1989**, *90*, 5622.

(33) Curtiss, L. A.; Raghavachari, K.; Redfern, P. C.; Pople, J. A. *J. Chem. Phys.* **1997**, *106*, 1063.

(34) Curtiss, L. A.; Redfern, P. C.; Raghavachari, K.; Pople, J. A. *J. Chem. Phys.* **1998**, *109*, 42.

(35) Curtiss, L. A.; Raghavachari, K.; Redfern, P. C.; Pople, J. A. *J. Chem. Phys.* **2000**, *112*, 7374.

(36) Curtiss, L. A.; Redfern, P. C.; Raghavachari, K.; Pople, J. A. *J. Chem. Phys.* **2001**, *114*, 108.

(37) Grimme, S. *J. Chem. Phys.* **2003**, *118*, 9095.

(38) Grimme, S. *J. Comput. Chem.* **2004**, *25*, 1463–1473.

(39) Grimme, S. *J. Phys. Chem. A* **2005**, *109*, 3067–3077.

(40) Zhao, Y.; Lynch, B. J.; Truhlar, D. G. *Phys. Chem. Chem. Phys.* **2005**, *7*, 43–52.

(41) Zhao, Y.; González-García, N.; Truhlar, D. G. *J. Phys. Chem. A* **2005**, *109*, 2012–2018.

(42) Zhao, Y.; González-García, N.; Truhlar, D. G. *J. Phys. Chem. A* **2006**, *110*, 4942–4942.

(43) Jurecka, P.; Sponer, J.; Cerny, J.; Hobza, P. *Phys. Chem. Chem. Phys.* **2006**, *8*, 1985–1993.